Optical Mode Control of Surface-Plasmon Quantum Cascade Lasers

V. Moreau, M. Bahriz, J. Palomo, L. R. Wilson, A. B. Krysa, C. Sirtori, D. A. Austin, J. W. Cockburn, J. S. Roberts, and R. Colombelli

***Abstract*—Surface-plasmon waveguides based on metallic strips can provide a two-dimensional optical confinement. This concept has been successfully applied to midinfrared quantum cascade lasers, processed as ridge waveguides, to demonstrate that the lateral extension of the optical mode can be influenced solely by the width of the device top contact. In this configuration, the waveguide mode has a reduced interaction with the top metal and the ridge sidewalls. This results in lower propagation losses and higher performances. For devices operating at a wavelength of $\lambda \approx 7.5$ μm, the room-temperature threshold current density was reduced from 6.3 to 4.4 kA/cm^2 with respect to larger devices with full top metallization.**

***Index Terms*—Midinfrared, semiconductor lasers, surface-plasmons.**

THE quantum cascade (QC) laser [1] has proven to be a promising midinfrared and terahertz laser source. It is now the semiconductor source of choice for the first and second atmospheric windows [2], [3]. In particular, the performance of these devices has rapidly progressed, thanks to better material qualities, and to the use of more advanced processing/packaging techniques, such as electroplating and InP regrowth [4]–[6].

Novel functionalities such as multiwavelength operation [7], broadband laser emission [8], and intracavity frequency conversion [9] have been achieved which are difficult to implement for conventional interband lasers. The possibility of employing metallic waveguides, based on surface-plasmons [10], is possible due to the transverse-magnetic polarization of intersubband transitions, on which QC lasers are based. While it is commonly assumed that surface-plasmon waveguides exhibit low propagation-losses at far-infrared wavelengths only [11], [12], it has been recently shown that low-loss metallic waveguides can also be implemented at midinfrared wavelengths [13].

Here we show that the lateral laser mode extension of surface-plasmon QC lasers can be controlled simply by acting on the width of the top contact dimension, in contrast to devices employing conventional waveguides in which the lateral mode dimension is typically determined by the etched laser ridge width. This phenomenon stems from the fact that the optical mode—in a surface plasmon QC laser—is a surface-plasmon wave bound at the top metal–semiconductor interface. The ability to confine the optical mode nearer the center of the ridge, away from the lossy sidewalls, reduces the threshold current density ($J_{\rm th}$) by $\sim$30% compared to surface plasmon QC lasers where the top contact extends across the whole width of the ridge. This technique might allow one to reduce to a minimum the laser ridge width—an important requirement for efficient heat dissipation—without a substantial loss increase.

The laser structure (MR2230) used here was grown by metal–organic vapor phase epitaxy, using an $In_{0.53}Ga_{0.47}As$–$Al_{0.48}In_{0.52}As$ lattice matched to a highly doped InP substrate. Further details of the growth process can be found in [14]. The active regions (two-phonon-resonance design, see [13] and [15]) are designed for emission at 7.5 μm.

The mode guiding properties of surface-plasmons suggest that the implementation of a planar technology (i.e., devices without an etched mesa) could be possible [16]. We therefore fabricated planar devices as follows: a 300-nm-thick layer of SiN was first deposited on the sample, and 8-12-16-20-μm-wide trenches where then opened via reactive-ion-etching (RIE). Ti–Au contacts were evaporated on the top surface of the devices, which were then cleaved (1 mm long) and mounted for optoelectronic characterizations. We observed that the turn-on of the current–voltage (I–V) characteristics (i.e., the applied bias where the QC structure is correctly aligned and current can flow with low differential resistance) is less pronounced when the opening is smaller. This behavior suggests that the current injection through an aperture in a planar device (i.e., without a mesa to confine current) is less effective if the aperture is reduced, due to competition between the vertical and the parallel conductivities. On one hand, for these fully planar devices, the current dispersion in the lateral direction was large enough to hinder the performances (the maximum operating temperature was only 200 K). On the other hand, in combination with an etched mesa, the current dispersion can be an advantage since it allows one to inject current through a contact which can be substantially smaller than the mesa surface. We obtained an estimate of the current spreading as follows. All the planar devices were operational; however, the current threshold at 78 K lies in a small range (between 1.45 and 1.7 A) for all the lasers, suggesting that the volume of the pumped region is defined essentially by the current spreading. If we assume that the $J_{\rm th}$ is $\approx 2.5/3$ kA/cm^2 (the typical $J_{\rm th}$ for surface-plasmon QC lasers fabricated with this material and Ti–Au contacts), we can infer the width of the pumped region, i.e., the sum of the *contact width + current spreading on each side*. We obtained an appffroximate value of $\approx 20/25$ μm per side, which is our estimate.

Manuscript received July 24, 2006; revised September 7, 2006. This work was conducted as part of a EURYI scheme award. This work was supported by the U.K. Engineering and Physical Sciences Research Council (EPSRC). The device fabrication was performed at the nano-center "Centrale Technologique Minerve" at the Institut d'Electronique Fondamentale.

V. Moreau, M. Bahriz, J. Palomo, and R. Colombelli are with the Institut d'Electronique Fondamentale- UMR8622 CNRS, Université Paris Sud, 91405 Orsay, France (e-mail: colombel@ief.u-psud.fr).

L. R. Wilson, D. A. Austin, and J. W. Cockburn are with the Department of Physics and Astronomy, University of Sheffield, Sheffield S3 7RH, U.K.

A. B. Krysa and J. S. Roberts are with the EPSRC National Centre for III-V Technologies, University of Sheffield, Sheffield, S1 3JD, U.K.

C. Sirtori is with the Université Denis Diderot Paris VII, 75005 Paris, and Thales Research and Technology, 91767 Palaiseau Cedex, France.

Color versions of Figs. 1–3 are available online at http://ieeexplore.ieee.org.

Digital Object Identifier 10.1109/LPT.2006.886827

1041-1135/$20.00 © 2006 IEEE

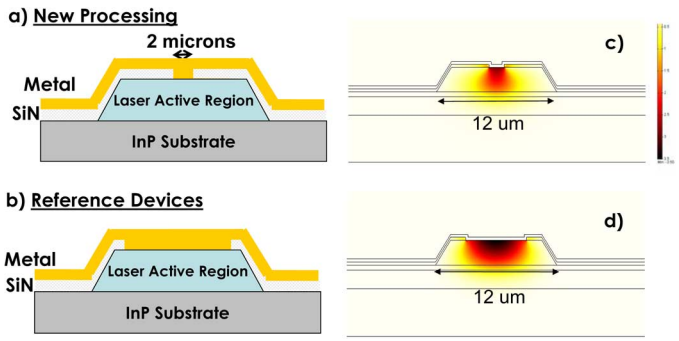

Fig. 1. (a) Scheme of the fabricated devices: a 2-μm-wide window is opened in the insulating SiN layer. The top contact is 2 μm wide for all the tested laser devices. (b) Schematic view of the reference devices (see [13]): the top contact covers the whole top surface of the laser ridge. (c) Two-dimensional simulation (see text for details[1]) of the waveguide mode for a 12-μm-wide ridge with a 2-μm-wide top contact. The optical mode lateral extension is controlled by the lateral top contact extension. (d) Two-dimensional simulation[1] of the waveguide mode for a 12-μm-large ridge with a 10-μm-wide top contact (reference devices).

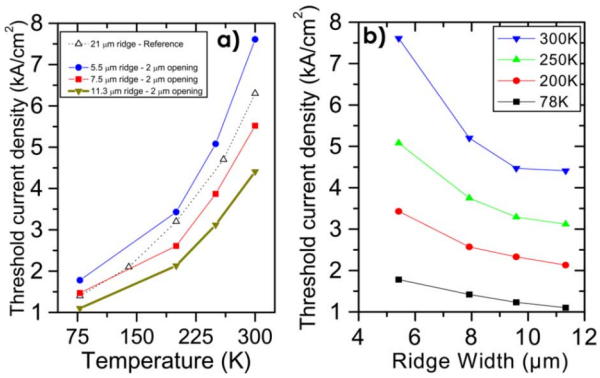

Fig. 2. (a) Threshold current density as a function of temperature for the devices with a 2-μm top opening (full lines), and for a reference device with full top metallization (dotted line). The devices with 2-μm openings feature the following ridge widths: 5.5, 7.5, 9.6, and 11.3 μm. The reference device is 21 μm wide. (b) Threshold current densities as a function of the ridge width, and for different operating temperatures, for the devices with 2-μm top openings.

It is clear, therefore, that—although the optical mode can be guided by the surface-plasmon-carrying metal strip—it is necessary to etch a ridge mesa in order to prevent an excessive lateral spreading of the injected current.

New lasers were, therefore, processed into a range of narrow, etched ridges (5.5, 7.5, 9.5, and 11.5 μm wide), following the procedure in [13]. A 300-nm-thick layer of Si_3N_4 was deposited to provide electrical insulation, and narrow (2 μm wide) windows were opened on top of the devices via fluorine-based RIE [Fig. 1(a)]. A Ti–Ag–Ni–Au contact (3/150/10/250 nm) was evaporated as top metallization. After mechanical polishing and back contact deposition, the samples were cleaved into laser bars, mounted with indium solder on copper blocks, wire-bonded, and loaded in a cryostat for device characterization.

In contrast, the reference devices in [13] were processed as larger laser ridges (13-17-21-24 μm wide), with a silver-based top contact layer extending on the whole ridge surface, as shown in Fig. 1(b).

Two-dimensional (2-D) numerical simulations[1] were performed. In the simulations, the index of refraction of the doped semiconductor layers was obtained through a Drude–Lorentz model, while the index of refraction for the metal layers was taken from the literature [17]. As for the SiN layer, we used a complex index of refraction $n = 1.7 + i*10^{-2}$. This corresponds to a value $\alpha = 170cm^{-1}$ for the transmission losses of SiN at $\lambda \approx 7.5$ μm [18]. The results show that the waveguide mode is bound to the top-metal interface [16]. Fig. 1(c) shows a 2-D simulation for the waveguide mode of a 12-μm-wide laser ridge with a 2-μm-wide top contact (i.e., the typical devices fabricated for this work). The mode is confined below the metallic strip only. On the other hand, when the top metallic strip is made almost as large as the ridge (like in the reference devices of [13]), then the optical mode is correspondingly larger. This situation is clarified by the simulation reported in Fig. 1(d), where the optical mode overlaps with the whole laser ridge volume.

[1]The simulations were performed with the commercial software package COMSOL Multiphysics. The solution to the wave equation was obtained with a finite-elements solver. The mesh was adapted to the geometry of the problem, i.e., a thin mesh was used for the metallic layers, while a sparser one was used for the semiconductor layers where the optical mode decays more slowly

The optical losses for this type of waveguides mainly originate from 1) the mode penetration into the top metal layer strip and from 2) the mode penetration into the lossy SiN and metal layers on the ridge sides. The device configuration exhibiting a narrow top contact is, therefore, particularly advantageous. Our simulations indicate that the lateral confinement of the mode induced by the narrow top contact (2 μm wide in our case), and especially the reduced interaction of the optical mode with the top metal significantly reduce the losses. We calculate the following values for the waveguide losses: $\alpha \approx 38$ cm^{-1} for a 20-μm-wide ridge with complete top contact Fig. 1(b) and $\alpha \approx 29$cm^{-1} for a 20-μm-wide ridge with reduced top metallization Fig. 1(a). If the mirror losses[2] are taken into account, for instance for a 1.5-mm-long device, we calculate a reduction of $\approx$20% of the threshold current density for a sample with a narrow top contact, with respect to a device with full top metallization.

The lasers were tested in pulsed mode (100-ns pulsewidth at 84 kHz for spectral measurements, and 75 ns at 5 kHz for light–current (L–I) characterizations). A liquid nitrogen cooled mercury cadmium telluride (MCT) detector was used for spectral analysis, and a fast, room-temperature (RT) MCT detector was employed to determine the output power. Fig. 2(a) reports the threshold current density for laser action ($J_{\rm th}$) as a function of temperature for the two different families of devices with narrow Fig. 1(a) and large [see [13] and Fig. 1(b)] top contacts. The current densities were calculated using the full area of the ridge in both cases. Since the ridge widths are well below the value we estimated for the current spreading in the fully planar devices, we expect that the injected current will pump the full volume of the ridge, even when it is injected from a narrow 2-μm-wide top contact. This hypothesis is corroborated by the I–V characteristics of a typical device (Fig. 3). The sharp turn-on of the I–V is a strong indication that the current is efficiently injected.

All the devices with the narrow top contact (except the narrowest ones) exhibit improved characteristics, especially at RT. At 78 K, the $J_{\rm th}$ was improved by 20%, in agreement with our

[2]The mirror losses were estimated using the following formula: $\alpha_m = -(1/L)\ln(R_1R_2)$, where L is the laser cavity length, and R_1, R_2 are the mirror reflectivity (approximately 0.3).

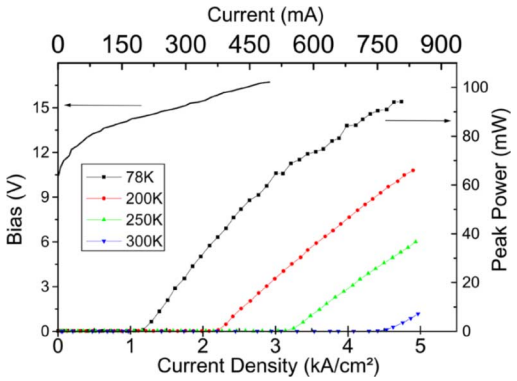

Fig. 3. L–I and I–V characteristics of an 11-μm-wide laser with a 2-μm-wide top metallic contact. The peak power at 78 K is $\approx$100 mW. The laser was operated in pulsed mode (75-ns pulsewidth, 5-kHz repetition rate). The signal was detected with an RT HgCdTe detector that has been calibrated with a thermopile.

calculations: from 1.4 kA/cm^2 in a 21-μm-wide laser with standard top contact, to less than 1.1 kA/cm^2 in a smaller 11-μm -wide device with a 2-μm-wide top contact. The effect is larger at RT, where the $J_{\rm th}$ correspondingly decreases from 6.3 to 4.4 kA/cm^2, i.e., 30%.

The threshold current density of the devices with narrow top metallization, as a function of the laser ridge width, is summarized in Fig. 2(b) for different operating temperatures. A rapid increase in $J_{\rm th}$ appears for a ridge width of $\sim$5.5 μm, especially at high temperatures (250 K and 300 K). This behavior proves that when the optical mode leaks into the ridge sidewalls—covered by SiN and metal—the propagation losses are increased. In addition, this behavior is more evident at 250/300 K, probably because of the change of the complex index of refraction of metals as a function of temperature [19], [20]. The same phenomenon is responsible for the stronger threshold reduction at RT than at 78 K. All this suggests that, in order to further reduce the ridge width without increasing the losses, a further decrease of the lateral extension of the optical mode is required. Finally, L–I and I–V characteristics of a typical device are reported in Fig. 3. For a laser 11 μm wide, a peak output power of almost 100 mW is obtained at 78 K. The slope efficiency at 78 K is $\approx$200 mW/A.

Concerning the reliability of these devices, the important issues are 1) the oxidation of silver and 2) the high contact resistance. The latter characteristic, which stems from the properties of the semiconductor/silver interface, prevented up to now the continuous-wave operation of the devices. The former characteristic instead affects their long-term stability. We observed that the silver oxidation tends to proceed inward from the contact edges (especially where SiN is present), even if the last evaporation step is a 300-nm-thick gold layer. While we did not observe particular problems while operating the devices in pulsed-mode, the oxidation might degrade the lasers with time. We plan to address this problem thanks to a different fabrication procedure. The silver layer will be completely "buried" below a thick Ti–Au contact from all sides, in order to avoid that an exposed edge can act as a starting point for the oxidation.

In conclusion, we have shown that control of the lateral extension of the laser mode of surface-plasmon QC lasers can be achieved by modifying the top contact dimensions. By using a narrow top contact metal stripe, we have reduced the RT threshold current by 30% compared to surface-plasmon QC lasers having complete surface metal coverage. Finally, the implementation of a fully planar technology for surface-plasmon QC lasers is at the moment hampered by current–dispersion issues, that could be solved in the future thanks to the use of ion-implantation techniques.

ACKNOWLEDGMENT

The authors would like to thank F. Julien, A. de Rossi, R. Teissier, and O. Painter for useful discussions, and S. David for technical support.

REFERENCES

[1] J. Faist, F. Capasso, D. L. Sivco, C. Sirtori, A. L. Hutchinson, and A. Y. Cho, "Quantum cascade laser," *Science*, vol. 264, pp. 553–556, 1994.
[2] C. Gmachl, F. Capasso, D. L. Sivco, and A. Y. Cho, "Recent progress in quantum cascade lasers and applications," *Rep. Progr. Phys.*, vol. 64, pp. 1533–1601, 2001.
[3] J. Faist and C. Sirtori, *Long Wavelength Infrared Semiconductor Lasers*. Hoboken, NJ: Wiley, 2004.
[4] M. Beck, D. Hofstetter, T. Allen, J. Faist, U. Oesterle, M. Ilegems, E. Gini, and H. Melchior, "Continuous wave operation of a mid-infrared semiconductor laser at room temperature," *Science*, vol. 295, pp. 301–305, 2002.
[5] J. S. Yu, S. Slivken, A. Evans, L. Doris, and M. Razeghi, "High-power continuous-wave operation of a 6 μm quantum-cascade laser at room temperature," *Appl. Phys. Lett.*, vol. 83, pp. 2503–2505, 2003.
[6] M. Troccoli, D. Bour, S. Corzine, G. Hofler, A. Tandon, D. Mars, D. J. Smith, L. Diehl, and F. Capasso, "Low-threshold continuous-wave operation of quantum-cascade lasers grown by metalorganic vapor phase epitaxy," *Appl. Phys. Lett.*, vol. 85, pp. 5842–5844, 2004.
[7] C. Gmachl, D. L. Sivco, R. Colombelli, F. Capasso, T. S. Mosely, A. Straub, J. N. Baillargeon, and A. Y. Cho, "Quantum-cascade lasers with heterogeneous cascades: Multiple-wavelength operation," *Opt. Photon. News*, vol. 12, pp. 24–26, 2001.
[8] C. Gmachl, D. L. Sivco, R. Colombelli, F. Capasso, and A. Y. Cho, "Ultra-broadband semiconductor laser," *Nature*, vol. 415, pp. 883–887, 2002.
[9] N. Owschimikow, C. Gmachl, A. Belyanin, V. Kocharovsky, D. L. Sivco, R. Colombelli, F. Capasso, and A. Y. Cho, "Resonant second-order nonlinear optical processes in quantum cascade lasers," *Phys. Rev. Lett.*, vol. 90, pp. 043902-1–043902-4, 2003.
[10] C. Sirtori, C. Gmachl, F. Capasso, J. Faist, D. L. Sivco, A. L. Hutchinson, and A. Y. Cho, "Long-wavelength (λ = 8–11.5μm) semiconductor lasers with waveguides based on surface plasmons," *Opt. Lett.*, vol. 23, pp. 1366–1368, 1998.
[11] R. Colombelli, F. Capasso, C. Gmachl, A. L. Hutchinson, D. L. Sivco, A. Tredicucci, M. C. Wanke, A. Sergent, and A. Y. Cho, "Far-infrared surface-plasmon quantum-cascade lasers at 21.5 μm and 24 μm wavelengths," *Appl. Phys. Lett.*, vol. 78, pp. 2620–2622, 2001.
[12] A. Tredicucci, C. Gmachl, F. Capasso, A. L. Hutchinson, D. L. Sivco, and A. Y. Cho, "Single-mode surface-plasmon laser," *Appl. Phys. Lett.*, vol. 76, pp. 2164–2166, 2000.
[13] M. Bahriz, V. Moreau, J. Palomo, R. Colombelli, D. A. Austin, J. W. Cockburn, L. R. Wilson, A. B. Krysa, and J. S. Roberts, "Room-temperature operation of λ =7.5 μm surface-plasmon quantum cascade lasers," *Appl. Phys. Lett.*, vol. 88, pp. 181103-1–181103-3, 2006.
[14] A. B. Krysa, J. S. Roberts, R. P. Green, L. R. Wilson, H. Page, M. Garcia, and J. W. Cockburn, "MOVPE-grown quantum cascade lasers operating at similar to 9 μm wavelength," *J. Cryst. Growth*, vol. 272, pp. 682–685, 2004.
[15] R. P. Green, L. R. Wilson, E. A. Zibik, D. G. Revin, J. W. Cockburn, C. Pflügl, W. Schrenk, G. Strasser, A. B. Krysa, J. S. Roberts, C. M. Tey, and A. G. Cullis, "High-performance distributed feedback quantum cascade lasers grown by metalorganic vapor phase epitaxy," *Appl. Phys. Lett.*, vol. 85, pp. 5529–5531, 2004.
[16] J. Alton, S. Dhillon, C. Sirtori, A. de Rossi, M. Calligaro, S. Barbieri, H. Beere, E. H. Linfield, and D. A. Ritchie, "Buried waveguides in terahertz quantum cascade lasers based on two-dimensional surface plasmon modes," *Appl. Phys. Lett.*, vol. 86, pp. 071109-1–071109-3, 2005.
[17] M. A. Ordal, L. L. Long, R. J. Bell, S. E. Bell, R. R. Bell, R. W. Alexander, Jr., and C. A. Ward, "Optical-properties of the metals AL, CO, CU, AU, FE, PB, NI, PD, PT, AG, TI, and W in the infrared and far infrared," *Appl. Opt.*, vol. 22, pp. 1099–1119, 1983.
[18] Z. Yin and F. W. Smith, "Optical dielectric function and infrared-absorption of hydrogenated amorphous-silicon nitride films – Experimental results and effective-medium-approximation analysis," *Phys. Rev. B*, vol. 42, pp. 3666–3675, 1990.
[19] E. Palik, *Handbook of Optical Constants of Solids*. New York: Elsevier Science, 1991.
[20] J. Jackson, *Classical Electrodynamics*. Somerset, NJ: Wiley, 1998.